



## Experimental study of the ultrafiltration for bi-disperse silica systems

Nor Hanuni Ramli<sup>a,b,\*</sup>, Paul Melvyn Williams<sup>a</sup>

<sup>a</sup>Multidisciplinary Nanotechnology Centre, Swansea University, Swansea, SA2 8PP, UK

<sup>b</sup>Faculty of Chemical Engineering and Natural Resources, Universiti Malaysia Pahang, Lebuhraya Tun Razak, 26300 Kuantan, Pahang, Malaysia

Tel. +447517230420; emails: norhanuni@yahoo.com; cewillpa@swansea.ac.uk

Received 20 October 2010; Accepted 9 October 2011

### ABSTRACT

The filtration rate in monodisperse colloidal systems has previously been predicted by taking into account the interactions between particles, interpreted in the form of an osmotic pressure. However, most membrane filtration applications deal with multi-component feeds, consisting of particles of different sizes. These polydisperse ultrafiltrations are poorly understood, largely due to the lack of adequate experimental data and the complexity of the system. These systems are also more difficult to interpret when compared to the single component feed systems. This work investigates the ultrafiltration of bi-disperse feed solutions of colloidal silica. Experimental studies were carried out on two different sized silica particles: X30 and W30. Feed solutions with a total silica concentration of 4 g l<sup>-1</sup> were prepared. These solutions consisted of a 0.03M NaCl electrolyte with the following mixing ratio of X30:W30 by weight: (i) 100% X30, (ii) 100% W30, (iii) 20%:80% (iv) 40%:60%, (v) 60%:40% and (vi) 80%:20%. The solutions were filtered at an applied pressure of 200 kPa, through a 4 kDa molecular weight cut-off membrane. The permeate flux versus time data was recorded at pH's 4, 6 and 9. At each pH, the variation of the permeate flux was observed and compared to the two monodisperse systems.

*Keywords:* Ultrafiltration; Polydisperse; Colloidal Interactions; Modelling; Cake Resistance; Colloidal Silica

### 1. Introduction

In the early stages of filtration modeling, the effects of particle interactions were neglected [1,2]. However for ultrafiltration and nanofiltration, these effects cannot be ignored as the charge effects become significant when predicting or measuring the rate of filtration for smaller solute sizes [3]. The filtration rate for monodisperse colloidal systems has previously been predicted by taking into account the interactions between particles,

interpreted in the form of an osmotic pressure [3–5]. However, most real solutions will contain a range of particle sizes, that is they are polydisperse, and the degree of polydispersity in the solution will also effect the interactions between particles and thus the filtration rate. Therefore, models for predicting the rate of filtration which take into account particle interactions and the degree of polydispersity are important in order to get closer predictions of flux decline with actual flux reduction. In this paper an experimental investigation of the filtration rate versus time is carried out for bidisperse colloidal silica particle suspensions.

\*Corresponding author.

## 2. Theoretical aspects

### 2.1. Concentration polarization theory

The relationship between the applied ultrafiltration pressure and the rate of permeation or the flux for a pure solvent feed flowing under laminar conditions in tortuous membrane channels was described by the Carman–Kozeny equation [6]:

$$J = \frac{|\Delta P|}{\mu R_m} \quad (1)$$

where  $J$  = the flux (volumetric rate per unit area),  $\Delta P$  = the transmembrane pressure difference,  $R_m$  = the membrane resistance and  $\mu$  = the pure solvent viscosity. Eq. (1) describes the flux for a pure solvent, however when a solute is present in the feed this needs to be taken into account. As a solution containing a solute is filtered, the retained solute causes the local concentration at the surface of the membrane to increase, an effect which is known as *concentration polarization*. This effect can be taken into account by modifying Eq. (1) in various ways to allow for the presence of the solute in the feed.

*Osmotic Pressure Model.* Eq. (1) can be modified by the subtraction of an osmotic pressure term,  $\Delta\pi$ , from the applied pressure.

$$J = \frac{|\Delta P| - |\Delta\pi|}{\mu R_m} \quad (2)$$

The osmotic pressure arises due to the build up of a concentrated layer of particles near the surface (i.e., concentration polarization) and reduces the driving force pushing the solute through the membrane, therefore reducing the membrane flux. This method is commonly used for low molecular weight solutes and colloids [7].

*Resistance Model.* In the basic flux equation (Eq. (1)), the flux is controlled by an applied pressure difference and membrane resistance. In the presence of a solute however, ultrafiltration performance can be interpreted by a resistance-in-series relationship [8],

$$J = \frac{1}{A_m} \left( \frac{dV}{dt} \right) = \frac{|\Delta P|}{\mu(R_m + R_s)} \quad (3)$$

with,

$$R_s = \frac{\alpha V C_b}{A_m} \quad (4)$$

where  $\alpha$  = the specific cake resistance,  $V$  = the total volume filtered,  $C_b$  = the bulk solution concentration and  $A_m$  = the membrane area. The relationship between Darcy's law and the Carman–Kozeny equation is used to express,  $\alpha$ , the specific resistance of the deposited mass [6] as:

$$\alpha = \frac{180}{\rho_p d_p^2} \left( \frac{1 - \varepsilon}{\varepsilon^3} \right) \quad (5)$$

where  $\varepsilon$  = void volume,  $\rho_p$  = the particle density and  $d_p$  = the mean particle diameter.

### 2.2. Effect of polydispersity on the system

So far the equations shown have been developed on the basis of the solution being filtered having a mono-disperse particle size distribution. Real solutions are unlikely to conform to this idealistic interpretation, therefore polydispersity of the particle sizes needs to be taken into account. Endo and Alonso have proposed a theoretical model of cake filtration in the laminar flow regime which is applicable to a cake consisting of non-spherical particles having a log-normal size distribution [9]. This results in an alteration of Eq. (5) to:

$$\alpha = \frac{180}{\rho_p} \frac{\kappa}{d_{vg}^2 \exp(4 \ln^2 \sigma_g)} \frac{(1 - \varepsilon)}{\varepsilon^3} \quad (6)$$

where  $\kappa$  = a shape factor (which is equal to 1 for spheres),  $d_{vg}$  = the geometric mean diameter of  $d_p$  on a number basis and  $\sigma_g$  = the geometric standard deviation. If the particles are monodisperse Eq. (6) becomes identical to Eq. (5).

For a bi-disperse dispersion,  $d_{vg}$  and  $\sigma_g$  can be calculated using:

$$d_{vg} = \exp \left( \frac{\sum n_i \ln d_{p_i}}{\sum n_i} \right) \quad (7)$$

$$\sigma_g = \exp \left( \sqrt{\frac{\sum n_i [\ln(d_i / d_{vg})]^2}{\sum n_i}} \right) \quad (8)$$

### 2.3. Particle–particle interactions and prediction of ultrafiltration rates

Colloidal interactions originate from various forces, the two most important being electrostatic repulsion of double layers and dispersion forces [10]. Entropic effects are also important. These interactions are responsible for strikingly influencing the transport properties of colloidal suspensions, such as gradient diffusivity and also viscosity, and the thermodynamic properties such as the osmotic pressure [3,4]. The osmotic pressure is a key property in ultrafiltration processes as it controls the spatial distribution of particles in the concentration polarized layer and hence the rate of permeation. A full account of the prediction of osmotic pressure and filtration rate for monodisperse colloidal systems is given elsewhere [3–5].

The particle interactions are incorporated into the predictions through the osmotic pressure and local voidage, which vary with position in the filter cake and time, depending on the local interparticle interactions.

Introducing polydispersity as well as colloidal interactions into filtration theory is a very complex process. The osmotic pressure prediction for a polydisperse system has previously been considered by Dickinson [11]. In general, the formulated model defined the osmotic pressure in terms of compressibility factor estimates from the summation of repulsive forces and the entropic pressure as proposed by the Evans–Napper model [12]. However, even the basic equations used for estimating the compressibility factor whilst considering inter-particle interactions are very complex [11].

McDonogh et al. introduced a method to describe the specific resistance of a filter cake which takes into account the effect of polydispersity in conjunction with charge effects [13]. The voids formed during the filtration process appear to enlarge with an increase in the particle size, increase in zeta potential and separation distance between the particles. McDonogh et al. reported that the calculated void size reasonably mimicked the trends observed from experiment but the calculated values were higher than the values obtained experimentally [13]. This was attributed to the filling of interstices effect, which has been neglected in the theoretical estimation. In addition, the property of the voids formed is also affected by the composition of solution. A minimum porosity was achieved in the volume fraction range of 0.25–0.5 for the smaller particles [13].

In this present work, experimental tests have been carried out on mixtures of two different sized silica particles, X30 and W30, at various pH values. Analysis of the cake formed will be made using the simplified models described by Eqs. (6)–(8). No attempt has been made to include the particle interactions into the equations, however, the effects of zeta potential may be seen from the results obtained.

### 3. Materials and methods

#### 3.1. Stock solutions

Sodium chloride electrolyte solutions were made by dissolving a weighed amount of sodium chloride, obtained from Fisons Scientific Equipment (Grade: Fisons AR), in high purity water (produced by a Millipore Elix 3 system) to make a solution of the required ionic strength. The ionic strength of the electrolyte used was verified from specific conductivity measurements performed using a Portec PI-8140 digital conductivity meter in connection with a Philips conductivity cell (type: 4550/60).

The colloidal particles used were W30 and X30 colloidal silica (purchased from Morrisons Gas Related

Products Ltd). These came as liquid dispersions with the following properties: concentration  $\approx$  30% by weight, dispersion medium  $\approx$  0.03M NaCl solution (plus other stabilizers) at pH  $\approx$  9.5, particle diameter X30  $\approx$  15 nm, W30  $\approx$  50 nm. The exact concentration of this stock solution was determined in the following manner. Five petri dishes were taken and weighed using an electronic balance (Mettler Toledo P303 Delta Range, accurate to  $\pm$ 0.001 g). A known amount of the stock silica solution was then added to each petri dish. The dishes were then placed in an oven set at 120°C and left overnight to dry. The dishes were then weighed again the following day and the difference between this new weight and the clean petri dish weight was found. This corresponds to the mass of dry silica in the solution. The mass wt.% was then found by dividing the weight of dry silica by the total solution weight. Finally, the average value of the five measurements was taken and used subsequently as the concentration of the stock silica solution. Dilutions of this stock solution were made by adding known amounts of 0.03M NaCl to a known mass of the stock silica solution. The pH of the final silica solution was adjusted to the desired value by the dropwise addition of NaOH and HCl (both of Grade: Fisons AR). The pH measurements were carried out using a Philips PW 9421 digital high precision pH meter (pH resolution 0.01) in connection with a Russell CMAWL/4/5 pH probe.

#### 3.2. Size measurements

Dynamic light scattering measurements were performed with a Malvern 4700 system (Malvern Instruments Limited, UK). The light source was an Argon laser operating with vertically plane polarised light at a wavelength of 488 nm. All the dynamic light scattering measurements were carried out at a low laser power ( $\sim$ 13.3 mW), so the results are not influenced by local heating of the samples which would be caused by use of a more powerful beam. The scattering angle used was 90°. The temperature of the samples was automatically kept at  $25.0 \pm 0.1^\circ\text{C}$ . Prior to each experiment, the measurement cell was flushed with high-purity water to remove dust in the cell. Dynamic light scattering measurements were performed on  $4\text{g l}^{-1}$  silica dispersions in 0.03M NaCl at various pH values. Only solutions containing 100% W30 or 100% X30 were used for these experiments. The data measured was analysed according to BS 3406 (1997) in order to determine the particle size.

#### 3.3. Zeta potential measurements

The same silica dispersions as used for the size measurements were used for the electrophoretic mobility measurements. Electrophoretic mobility measurements

were made using a Zetasizer 2000 (Malvern Instruments, UK). Electrophoretic mobility values were converted to zeta-potentials using the WinMobil programme (Department of Mathematics, University of Melbourne) which is an extended implementation of an advanced theory of electrophoresis [14].

### 3.4. Filtration experiments

Filtration experiments were conducted using a membrane rig which was comprised of a nitrogen gas supply, filtration unit cell, balance and computer as shown in Fig. 1.

Filtration measurements were carried out using a 50 ml filtration cell (Amicon Corp., Model 8050) connected to a reservoir with a maximum capacity of 250 ml. The effective membrane area was 13.4 cm<sup>2</sup>. The system was pressurised with nitrogen gas and the cell was not stirred. The temperature of the system was kept constant at 25.0 ± 0.1°C via a water jacket on the filtration cell and a water bath around the reservoir. The filtration time was coupled to the amount of permeate collected—experiments were stopped usually after 25–30 ml of permeate was collected. The total filtration time was therefore in the range of 1–3 h, depending on the solution conditions. Rates of filtration were determined by continuously weighing the filtrate on an electronic balance connected to a micro-computer.

NADIR polyethersulphone membranes of molecular weight cut-off 4000D were obtained from MICRODYN-NADIR GmbH (Germany). Before use the membrane was cleaned using pure water and then soaked for at least 16 h. The hydraulic resistance of the NADIR 4000D membrane discs was determined by filtration of pure electrolyte solution through the membrane. The clean water flux or solvent flux rates are determined by filtering the water/electrolyte alone through a fresh membrane at five different pressures (50, 100, 200, 300 and 400 kPa) until 20 ml of permeate sample is collected at each pressure. The membrane resistance was calculated from the water flux measurements and Eq. (1).

Filtrations were then carried out on silica solutions containing a total silica concentration of 4g l<sup>-1</sup>.

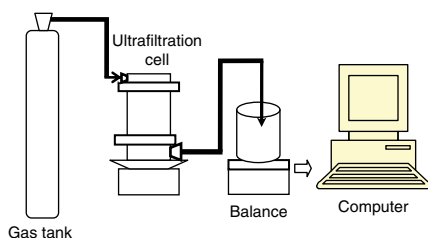


Fig. 1. Schematic diagram for simple filtration unit experimental set-up.

These solutions consisted of a 0.03M NaCl electrolyte with the following mixing ratio of X30:W30 by weight: (i) 100% X30, (ii) 100% W30, (iii) 20%:80% (iv) 40%:60%, (v) 60%:40% and (vi) 80%:20%. The filtration experiments were repeated at least three times to confirm the validity of the experimental data.

## 4. Results and discussion

### 4.1. Size and zeta potential measurements

The particle size and zeta potential results are shown in Table 1 for the X30 and W30 colloidal silica. Table 1 shows that W30 is approximately 3.3 times the size of X30. Ten measurements were made on each sample at pH 4, 6 and 9 and the average of all these measurements are shown in Table 1, as there is no appreciable difference in size between the measurements made at the three different pH values.

Table 1 also shows the zeta potentials measured at the different pH values. The zeta potential values are an average of at least 35 measurements on each sample. The zeta potential of W30 at pH 9 is appreciably higher than the value for X30 (~ 10mV), whilst at pH 6 the values are similar.

### 4.2. Filtration experiments

Fig. 2 shows the normalized results for the binary mixtures of X30 and W30 silica at pH 9. Normalized data is obtained by eliminating the effect of the hydraulic membrane resistance of the clean membrane, which is determined from the flux rate of the clean membrane using the electrolyte alone. As can be seen from Fig. 2 the fastest filtration is given by 100% composition of W30. The slowest filtration rate was exhibited by the 100% composition of X30. The rate of filtration decreased gradually as the amount of X30 added increased. Therefore, the rate of filtration became slower as the quantity of the smaller sized particles increased. In this case, as the zeta potential for both types of silica particle is very high (>80 mV), the filtration is controlled by the interactions between the particles rather than the way in which

Table 1

Size and zeta potential results for X30 and W30 colloidal silica in a 0.03M NaCl electrolyte solution (the ± values show the standard deviation away from the average value)

	X30	W30	
Particle Diameter (nm)	15.59 ± 0.91	51.64 ± 1.67	
Zeta Potential (mV)			
	pH 4	-15.9 ± 1.4	-7.2 ± 1.2
	pH 6	-29.4 ± 3.3	-29.8 ± 1.4
	pH 9	-89.3 ± 5.9	-98.3 ± 7.3

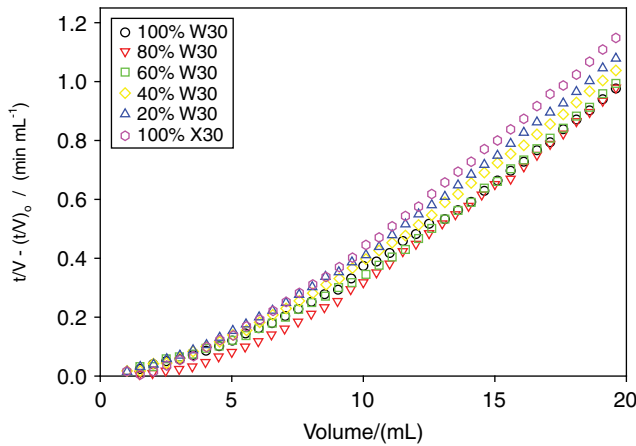


Fig. 2. Normalized flux for the filtration of silica binary mixtures (X30 and W30) at pH 9.0.

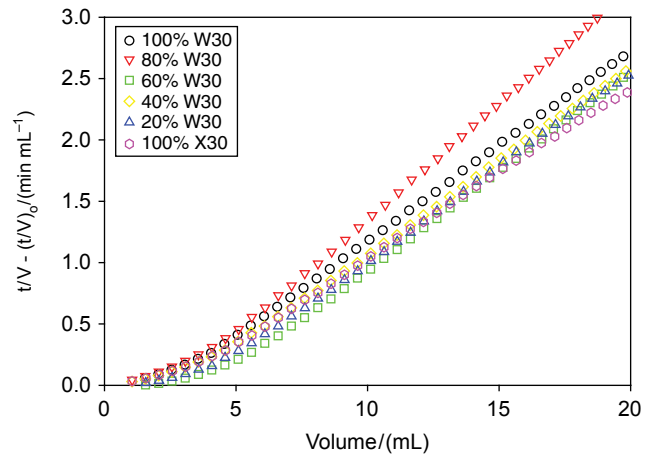


Fig. 3. Normalized flux for the filtration of silica binary mixtures (X30 and W30) at pH 6.0.

the particles pack. This is because the particles are being kept farther apart by the increased electrostatic interactions between them for both X30 and W30.

Fig. 3 shows the normalized results for the binary mixtures of X30 and W30 silica at pH 6. A different pattern of filtration rates is seen in this case. The fastest filtration is given by 100% composition of X30. The filtration rate of W30 is slower but is not the slowest value seen. When a small amount of X30 is added to W30, that is 20% by weight, the filtration rate of this solution is markedly slower than the filtration rates of 100% W30 and 100% X30. This is likely to be due to the filling of interstices in W30 filter cake in the bidisperse mixture [13]. The smaller X30 particles are filling in the gaps in the predominantly W30 filter cake, thus causing an increase in filter cake resistance and therefore reducing the rate of filtration. In this case, as the zeta potentials of the particles are comparable and much smaller than at pH 9, the filtration rate is controlled by the packing of the particles rather than the particle interactions. As the amount of X30 in the feed solutions increase from 20% X30 then the filtration rate tends towards the rate for 100% X30. There is likely to be a feed solution composition above which the amount of X30 dominates the filtration rate.

Fig. 4 shows the normalized results for the binary mixtures of X30 and W30 silica at pH 4. The 100% W30 and 100% X30 give similar filtration rates in this case. Again, as with the data at pH 6, addition of a small amount of X30 to the feed solution causes a sharp decrease in the filtration rate, most likely due to the reasons as discussed for pH 6. The 80% and 60% by weight W30 feed solutions give similar slow filtration rates, whilst the 40% and 20% by weight W30 feed solutions gave intermediate filtration rates between the extremes.

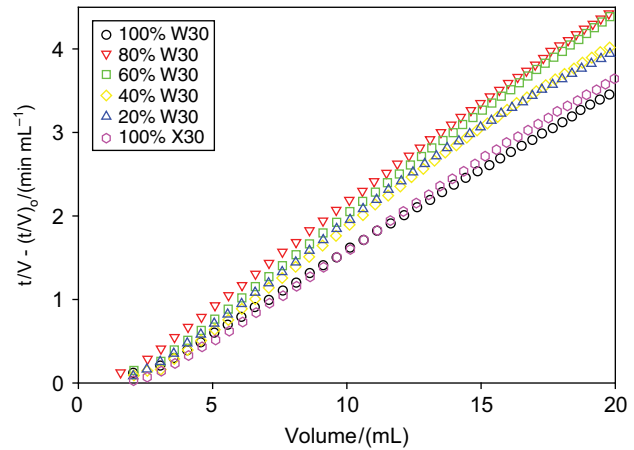


Fig. 4. Normalized flux for the filtration of silica binary mixtures (X30 and W30) at pH 4.0.

#### 4.3 Cake voidage

For illustration purposes the classical constant pressure filtration model [6]:

$$\frac{t}{V} = \frac{\mu R_m}{A_m \Delta P} + \frac{\mu C_b \alpha}{2 A_m^2 \Delta P} V \quad (9)$$

will be used to analyse the filtration data. For each filtration experiment, the cake voidage can be calculated by applying Eqs. (5)–(8) in conjunction with Eq. (9). The gradient of a graph of  $t/V$  versus  $V$  (or in this case  $[t/V - (t/V)_0]$  versus  $V$ ) yields:

$$\text{Gradient} = \frac{\mu C_b \alpha}{2 A_m^2 \Delta P} \quad (10)$$

Therefore, taking the gradients from the lines shown in Figs. 2–4 will give a value of  $\alpha$  for each experiment.

Table 2

Calculated voidage values for filter cakes of silica binary mixtures (X30 and W30) at various pH values in a 0.03M NaCl electrolyte solution

Sample	$d_{vg}$ nm	$\sigma_g$	$\alpha$ pH 9 $\times 10^{15}$ m kg <sup>-1</sup>	$\alpha$ pH 6 $\times 10^{15}$ m kg <sup>-1</sup>	$\alpha$ pH 4 $\times 10^{15}$ m kg <sup>-1</sup>	$\epsilon$ pH 9	$\epsilon$ pH 6	$\epsilon$ pH 4
100%W30	51.64	1.00	0.78	1.91	2.46	0.303	0.228	0.215
80%W30	17.56	1.43	0.83	2.30	3.00	0.467	0.354	0.329
60%W30	16.35	1.26	0.82	2.03	3.04	0.523	0.414	0.372
40%W30	15.93	1.17	0.83	1.94	2.88	0.544	0.439	0.395
20%W30	15.72	1.10	0.85	1.97	2.87	0.552	0.447	0.405
100%X30	15.59	1.00	0.91	1.70	2.71	0.549	0.471	0.418

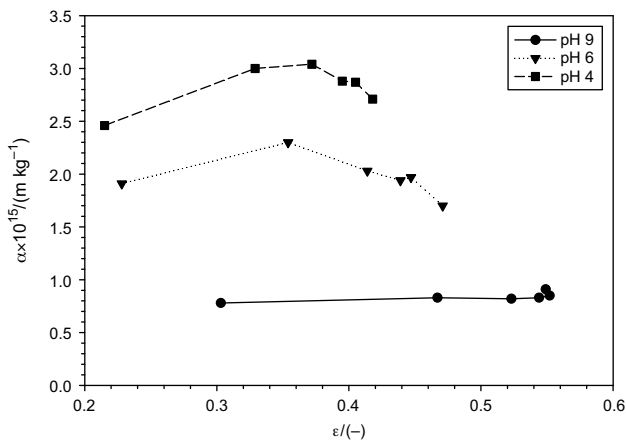


Fig. 5. Comparison of cake resistance versus voidage for polydisperse particles at different pH values.

These  $\alpha$  values can then be used with either Eq. (5) for monodisperse systems or Eqs. (6)–(8) for polydisperse systems in order to give the cake voidage. These results are shown in Table 2.

For monodisperse systems (100% W30 and 100% X30), Table 2 shows that the voidage in the cake decreases as the pH value decreases. This is as expected as the zeta potential reduces as the pH value reduces, meaning that the repulsive interactions between the particles become less resulting in a more dense filter cake (smaller voidage) and thus slower filtration rate. This pattern is also observed with mixtures of particles. The way in which particle polydispersity affects the voidage and thus cake resistance is shown in Fig. 5.

Fig. 5 shows the effects of zeta potential and degree of polydispersity on the system. Moving from left to right in Fig. 5, the composition of the solution changes from 100% W30 down to 0% W30. For the highest pH (i.e. pH 9) and thus the highest magnitude of zeta potential, there seems to be little effect of composition on the overall cake resistance. In this case the particles

are kept far apart in relative terms, by the particles interactions and thus the filter cake maintains a fairly constant resistance. However, as the pH and the magnitude of the zeta potential drops, the cake resistance goes through a maximum. This maximum occurs at a voidage of approximately 0.35 for both the pH 6 and pH 4 experiments and corresponding approximately to a 80% W30, 20% X30 mixture. In these cases there seem to be enough smaller particles in the system to start filling the gaps in the filter cake between the bigger particles, thus increasing the cake resistance to a maximum value. These results show the importance of the composition of the feed solution in terms of small and large particles. The peak becomes more pronounced as the magnitude of the zeta potential of the particles decreases.

## 5. Conclusions

This article has investigated the effect of particle size and particle interactions on the rate of filtration of bidisperse colloidal silica systems. For highly charged particles the filtration rate is controlled by the interactions between the particles whereas for more moderately charged systems the packing of particles is more important in that smaller particles fill in the voids between larger ones thus making the filtration slower. The results indicate that there is a certain combination of big and small particles which give the worst filtration performance for these systems. The results also show that modelling of these systems is going to be a complex process.

## Symbols

$A_m$	—	cross-sectional area of membrane surface (m <sup>2</sup> )
$C_b$	—	solution feed concentration (kg m <sup>-3</sup> )
$d_p$	—	mean particle diameter (m)
$d_{p,i}$	—	mean particle diameter of particle $i$ (m)
$d_{vg}$	—	geometric mean diameter (m)

$J$	—	permeation rate (flux) ( $\text{m s}^{-1}$ )
$n_i$	—	number of particles of type $i$ (-)
$\Delta P$	—	pressure difference ( $\text{N m}^{-2}$ )
$R_m$	—	resistance of Membrane ( $\text{m}^{-1}$ )
$R_s$	—	resistance due to solute ( $\text{m}^{-1}$ )
$t$	—	filtration time (s)
$V$	—	volume filtered ( $\text{m}^3$ )

#### Greeks

$\alpha$	—	specific resistance of the deposited mass ( $\text{m}^{-2}$ )
$\kappa$	—	shape factor (=1 for spheres) (-)
$\varepsilon$	—	fractional cake voidage at the membrane surface (-)
$\mu$	—	viscosity of the solvent ( $\text{kg m}^{-1} \text{sec}^{-1}$ )
$\Delta\pi$	—	osmotic pressure ( $\text{N m}^{-2}$ )
$\rho_p$	—	density of particle (=2,200 $\text{kg m}^{-3}$ for silica) ( $\text{kg m}^{-3}$ )
$\sigma_g$	—	geometric standard deviation (-)

#### References

- [1] J.J.S. Shen and R.F. Probst, On the prediction of limiting flux in laminar ultrafiltration of macromolecular solution, *Ind. Eng. Chem. Fund.*, 16(4) (1977) 459–465.
- [2] J.G. Wijmans, S. Nakao and C.A. Smolders, Flux limitation in ultrafiltration: osmotic pressure model and gel-layer model, *J. Membr. Sci.*, 20 (1984) 115–124.
- [3] W.R. Bowen and F. Jenner, Dynamic ultrafiltration model for charged colloidal dispersions: a Wiegner-Seitz cell approach, *Chem. Eng. Sci.*, 50(11) (1995) 1707–1736.
- [4] W.R. Bowen and P.M. Williams, Dynamic ultrafiltration model for proteins: a colloidal interaction approach, *Biotechnol. Bioeng.*, 50 (1996) 125–135.
- [5] W.R. Bowen and P.M. Williams, quantitative predictive modelling of ultrafiltration processes: colloidal science approaches, *Adv. Colloid Interface Sci.*, 134–135 (2007) 3–14.
- [6] P.C. Carman, *Fundamental principles of industrial filtration*, *Trans. Am. Inst. Chem. Eng.*, 16 (1938) 168–188.
- [7] O. Kedem and A. Katchalsky, Thermodynamic analysis of the permeability of biological membranes to non-electrolytes, *Biochim. Biophys. Acta*, 27 (1958) 229–246.
- [8] J.M. Coulson and J.F. Richardson, *Chemical Engineering*. 4th edn, Pergamon Press, Oxford, UK, 1991.
- [9] Y. Endo and M. Alonso, Physical meaning of specific cake resistance and effects of cake properties in compressible cake filtration, *Filtr. Separ.*, (2001) 43–46.
- [10] R.J. Hunter, *Foundation of Colloid Science*. 2nd edn, Oxford University Press, UK, 2001.
- [11] E. Dickinson, Polydispersity and osmotic pressure of stable ordered colloidal dispersions, *J. Chem. Soc. Faraday Trans.*, 75(2) (1979) 466–473.
- [12] R. Evans and D.H. Napper, Disjoining pressures in colloidal dispersions, *J. Colloid Interface Sci.*, 63 (1978) 43–48.
- [13] R.M. McDonogh, A.G. Fane, C.J.D. Fell and H.C. Flemming, The influence of polydispersity on the hydraulic behaviour of colloidal fouling layers on membranes perturbations on the behaviour of the “ideal” colloidal layer, *Colloids Surf. A: Physicochem. Eng. Aspects*, 138 (1998) 231–244.
- [14] R.W. O'Brien and L.R. White, Electrophoretic mobility of a spherical colloidal particle, *J. Chem. Soc. Faraday Trans. II*, 74 (1978) 1607–1626.
- [15] S.R. Wickramasingha, S.E. Bower, Z. Chena, A. Mukherjee and S.M. Husson, Relating the pore size distribution of ultrafiltration membranes to dextran rejection, *J. Membr. Sci.*, 340 (2009) 1–8.